International Journal of Robotics and Control Systems
Vol. 5, No. 6, 2025, pp. 3284-3299
ISSN 2775-2658
http://pubs2.ascee.org/index.php/ijrcs

A Peak-Centric Approach to Bearing Fault Diagnosis Using Progressive Moving Transform and 2D- Convolutional Neural Network

Abdelhafid Benyounes [a,1], Rabah Mokhtari [b,2], Imad Eddine Tibermacine [c,3,*], Abdelaziz Rabehi [d,4], Alfian Ma'arif [e,5]

[a] Electrical Engineering Laboratory (LGE), Department of Electrical Engineering, University of M'sila, PO Box 166, Ichbilia, 28000, M'sila, Algeria
[b] Computer Science Department, Faculty of Mathematics and Computer Science, University of M'sila, PO Box 166, Ichbilia, 28000, M'sila, Algeria
[c] Department of Computer, Automation and Management Engineering, Sapienza University of Rome, Via Ariosto, 25, 00185 Roma (RM), Rome, Italy
[d] Laboratory of Telecommunications and Smart Systems, Faculty of Sciences and Technologies, University of Djelfa, BP 3117, Djelfa, 17000, Algeria
[e] Department of Electrical Engineering, Universitas Ahmad Dahlan, Yogyakarta, Indonesia
[1] Abdelhafid.benyounes@univ-msila.dz; [2] rabah.mokhtari@univ-msila.dz; [3] tibermacine@diag.uniroma1.it;
[4] rab_ehi@hotmail.fr; [5] alfian.maarif@te.uad.ac.id
* Corresponding Author

ARTICLE INFO

Article history
Received October 06, 2025
Revised November 18, 2025
Accepted December 27, 2025

Keywords
Bearing Fault Diagnosis;
Progressive Moving Average Transform;
2D Convolutional Neural Network;
Peak Detection;
Vibration Signal Analysis;
Condition Monitoring

ABSTRACT

Bearing fault diagnosis is critical for predictive maintenance in industrial machinery, yet many existing data-driven methods struggle to adapt to varying operational loads and often analyze entire vibration signals, which can dilute key fault indicators. To address this, we propose a novel peak-centric approach that focuses on diagnostically rich signal regions, combining the Progressive Moving Average Transform (PMAT) with a 2D Convolutional Neural Network (CNN) for enhanced classification. Our primary contribution is a novel methodology that leverages localized peak regions for fault diagnosis, integrating the recently developed PMAT signal transformation and validating its generalization to mechanical systems to create highly discriminative 2D image representations from 1D vibration data. The method involves three key steps: extracting fixed-length signal fragments containing significant peaks, converting these fragments into 120×120 pixel images using the Left PMAT transform, and classifying the images into one of four health states using a custom 2D-CNN architecture. The model was rigorously evaluated on the CWRU dataset under a leave-one-load-out cross-validation scheme across four distinct load scenarios. It achieved exceptional performance, with macro-average F1-scores exceeding 99.83% in three of the four scenarios, specifically under loaded conditions (1-3 HP), and a top accuracy of 99.96%. A comparative analysis demonstrated that our PMAT-based method consistently outperformed a Continuous Wavelet Transform (CWT) baseline and other recent state-of-the-art models under these loaded scenarios. In conclusion, the proposed PMAT and 2D-CNN framework provides a robust and highly accurate tool for bearing fault diagnosis, successfully demonstrating PMAT's cross-domain generalization capability while establishing a competitive benchmark for future research. Future work will explore a hybrid PMAT-CWT transformation to further improve performance under zero-load conditions.

1. Introduction

The classification of bearing signal faults is a critical area of research in machinery fault detection and diagnosis, as bearings are fundamental components in rotating machinery across various industrial and transportation applications [1]. Faults in bearings can lead to significant operational inefficiencies, costly downtime, and potential safety hazards. The importance of bearing fault diagnosis extends across diverse sectors including aerospace, automotive, industrial manufacturing, railway, and energy applications, where effective fault detection can contribute to preventive maintenance, catastrophic accident prevention, and extended equipment service life [2], [3].With the advent of Industry 4.0, the integration of advanced machine learning and deep learning techniques has revolutionized fault detection, enabling more accurate and automated diagnostics.

Conventional methods for bearing fault detection have relied heavily on signal processing techniques, such as time-domain, frequency-domain, and time-frequency-domain analyses. Techniques like Fast Fourier Transform (FFT), Wavelet Transform (WT), and Empirical Mode Decomposition (EMD) have been widely used to extract features from vibration signals. However, these methods often require manual feature extraction and expert knowledge, making them time-consuming and prone to human error [4]. Additionally, many existing intelligent data-driven fault diagnosis techniques struggle to adapt to different working conditions such as varying motor loads or rotational speeds. Their performance can degrade when dealing with non-stationary or noisy signals, highlighting a key limitation of traditional machine learning approaches which rely on handcrafted features that must be decided a priori through trial and error [4], [5].

Deep learning (DL) has emerged as a powerful tool for fault detection due to its ability to automatically learn hierarchical features from raw data. Among DL techniques, Convolutional Neural Networks (CNNs) have shown exceptional performance in image processing and have been adapted for fault classification tasks. CNNs are particularly effective in extracting spatial features, making them suitable for analyzing 2D representations of vibration signals. Hybrid models that combine CNNs for feature extraction with classical machine learning classifiers, such as Support Vector Machines (SVMs), have also been proposed to enhance fault classification accuracy [6]. This adaptability has produced fruitful results in fields like image processing, speech recognition, and fault detection. Transforming 1D vibration signals into 2D representations has gained traction in recent years. This approach allows CNNs to capture both temporal and frequency-domain features, improving fault classification accuracy. Advanced approaches employ multimodal fusion by combining STFT images with time series data, using different neural network architectures for each modality and applying decision-level fusion through weighted averaging [7]. Other methods, such as hybrid signal processing, enhance feature extraction and reduce domain shifts between simulated and real-world data [8] while advanced noise reduction techniques, such as improved IEMD-based methods, generate low-noise time-frequency images that maintain fault-relevant information [9]. These preprocessing approaches demonstrate exceptional resilience to noise, achieving substantial accuracy improvements up to 15% in severe noise conditions [10].

While CNNs combined with 2D transformations have demonstrated high accuracy, challenges remain. Many existing methods rely on predefined transformations that may not adapt well to varying signal characteristics. For example, dimensionality reduction and optimization techniques, while addressing computational efficiency, may still result in high input data dimensions [11]. There is a need for innovative transformation techniques that are computationally efficient and capable of capturing progressive signal variations effectively while also handling noise. This work investigates the generalizability of the recently proposed Progressive Moving Transform (PMAT) [12] by applying it, for the first time, to mechanical fault diagnosis. The participation of one of PMAT's co-developers in this work provides firsthand methodological expertise, ensuring the faithful adaptation of the technique to this new domain. Our contributions are twofold: (1) We introduce a novel, peak-centric bearing fault diagnosis framework that integrates PMAT with a 2D convolutional neural network (2D-CNN), achieving superior performance under loaded operating conditions. (2) We offer a rigorous validation of PMAT's cross-domain applicability, demonstrating that its

performance is strongly influenced by the presence of well-defined signal peaks, a key insight for guiding future research and applications. Taking advantage of the strengths of both PMAT and CNNs, the proposed method aims to overcome the challenges of traditional and existing DL-based approaches. Another important point is that this paper focuses on signal fragments characterized by the presence of peaks, as these regions are more strongly influenced by the existence of faults. This idea was inspired by the first use of PMAT for heartbeat classification in the work [12]. The integration of advanced signal transformation techniques like PMAT with CNNs represents a promising direction for bearing fault classification. This review of the literature highlights the evolution of fault detection methods, the advantages of deep learning, and the gaps in existing approaches, providing a strong foundation for the proposed methodology.

The remainder of this paper is organized as follows: Section 2 presents a review of the related works and the foundational methodologies in bearing fault diagnosis. Section 3 highlights the main techniques used. Section 4 describes the dataset, the different scenarios and experiments adopted, and provides an overview of the proposed method and the CNN model architecture. Section 5 discusses the results obtained and compares them with recently published works. Finally, Section 6 concludes the paper with a general conclusion.

2. Related Works

The domain of bearing fault diagnosis has undergone a significant evolution, transitioning from traditional signal processing and machine learning techniques to sophisticated deep learning and transfer learning paradigms. Early methodologies were heavily reliant on expert-driven feature extraction. Techniques such as Empirical Mode Decomposition (EMD) [42], Tunable Q-factor Wavelet Transform (TQWT) [45], [46] and spectral analysis were employed to decompose and analyze vibration signals. The features manually extracted from these processes were then fed into classifiers like Support Vector Machines (SVM) [6], [44] and Adaptive Neuro-Fuzzy Inference Systems (ANFIS) for fault identification [27], [32]. While foundational, these approaches were limited by their dependence on domain expertise and often struggled with generalization across varying operational conditions and noise [5], [25].

The advent of deep learning (DL) marked a paradigm shift, enabling end-to-end Intelligent Fault Diagnosis (IFD) that automates feature learning directly from raw data [30], [32], [58]. Convolutional Neural Networks (CNNs) have been particularly dominant in this revolution. Early applications involved 1D-CNNs processing raw vibration signals [19], [21], [22], [53] and 2D-CNNs analyzing time-frequency representations like Continuous Wavelet Transforms (CWT) [35], [57], [59], [60]. To enhance feature representation and model performance, researchers have developed increasingly complex architectures. This includes deep residual networks (ResNet) to overcome training difficulties in very deep models [24], [31], [55], [56] and hybrid models that fuse CNNs with recurrent networks like Long Short-Term Memory (LSTM) and Gated Recurrent Units (GRU) to capture both spatial and temporal characteristics of vibration data [18], [34], [52]. The integration of attention mechanisms, such as Efficient Channel Attention (ECA) [7], has further improved diagnostic accuracy by enabling the model to focus on the most discriminative fault-related features, thereby enhancing robustness in noisy environments [15], [28].

A critical challenge in real-world applications is the scarcity of labeled fault data and the class imbalance between healthy and faulty states. To address this, generative deep learning models have been widely adopted for data augmentation. Variational Autoencoders (VAE) [1], [20] and Generative Adversarial Networks (GANs) [48]-[51] can synthesize high-quality fault samples, which helps in building balanced datasets and training more robust diagnostic models [1], [23]. Furthermore, the issue of domain shift-where a model trained under one set of operating conditions fails under another has been a major focus. Transfer Learning (TL) and domain adaptation techniques have been developed to bridge this gap. These methods leverage knowledge from a labeled source domain to perform accurate diagnosis in a different, unlabeled target domain, significantly improving model generalizability across different machines, loads, and speeds [26], [29], [33], [36], [43], [54].

Current research frontiers are exploring several advanced directions. Graph Neural Networks (GNNs) are being applied to model the structural relationships and non-Euclidean geometry within sensor data [2], [37]-[41]. There is also a growing emphasis on explainable AI (XAI) to interpret the decision-making process of DL models, moving them from "black boxes" to trustworthy systems [32]. The development of highly generalized models trained on simulated data that can perform accurately across a wide range of bearing designs represents another promising avenue [8]. Finally, comprehensive reviews continue to map the landscape, offering roadmaps for future research in areas like fault severity assessment [47] and the application of unsupervised and semi-supervised learning [20], [32], [43].

In summary, the field has progressed from manual, expert-dependent analyses to data-driven, automated deep learning systems. Current efforts are focused on enhancing the robustness, generalizability, and interpretability of these systems to meet the demands of real-world industrial applications. This work builds upon this solid foundation, particularly drawing from advancements in hybrid architectures, data augmentation, and transfer learning to develop a more effective and reliable fault diagnosis framework.

3. Method

3.1. Progressive Moving Average Transform

The Progressive Moving Average Transform (PMAT) transform is a new published method proposed to convert 1D discrete signals to 2D representation [12]. The computational complexity of the PMAT algorithm is $O(N^2)$, where N is the length of the input signal. For comparison, the Continuous Wavelet Transform (CWT) typically exhibits a complexity of $O(N \times S)$, where S is the number of scales; when a large number of scales is used, its overall complexity also approaches $O(N^2)$. The authors of this new method have used it together with a Convolutional Neural Network (CNN) to classify heartbeats on the electrocardiogram (ECG). The method exhibited high performance for the classification of these kinds of signals. The PMAT transform is defined in three variants, left, right, and center PMAT. The Left PMAT (LPMAT) used in our paper is defined in.

$$LPMA(X,k,\omega) = \begin{cases} MA(X,1,\omega) & if k \leq \omega \\ MA(X,k-\omega+1,w) & otherwise \end{cases} \quad (1)$$

where X and w represent, respectively, the discrete signal and the window size. MA is the moving average defined as follows.

$$MA(X,j,\omega) = \frac{\sum_{i=j}^{j+w-1}(X_i)}{\omega} \quad (2)$$

The Sub-figures (B) and (C) of Fig. 1 represent, respectively, a fragment of length 6×10^{-1} second extracted from the accelerometer drive end signal OR021@6_0 sampled at 12 kHz of the CWRU bearing database and its PMAT transform.

3.2. Peak Detection

Unlike many studies that focus on analyzing whole signals, we believe that bearing faults can be captured more effectively in specific regions of the signal. Therefore, our study concentrates on the signal segments that contain significant peaks. To extract these regions, we used the *find_peaks()* function from the SciPy library with the parameter *distance*=100, which enforces a minimum separation of 100 samples between consecutive peaks. The *height* and *prominence* parameters were not constrained, as the signal amplitude was already normalized and visually inspected to ensure that only relevant peaks were detected. The distance value was empirically chosen based on the typical temporal spacing between significant waveform events in our signals. Sub-figure (A) of Fig. 1 shows the first 8 extracted peaks from the first 10^{-1} seconds of the OR021@6_0 signal sampled at 12 kHz of the CWRU bearing database.

4. Bearing Fault Classification Using 2D-CNN Model and PMAT Transform

4.1. CWRU Dataset

The Case Western Reserve University (CWRU) Bearing Fault Dataset is a benchmark dataset widely used for the development and validation of algorithms for bearing fault detection and diagnosis. The data comprises vibration signals collected from a mechanical test rig under both normal and fault-induced conditions.

Data was acquired from a driven mechanical system consisting of a 2 hp Reliance Electric motor, a torque transducer, and a dynamometer, as shown in Fig. 2. Vibration data was recorded using accelerometers attached to the housing with magnetic bases. Data was collected at two primary locations: at the fan end of the motor housing and at the drive end of the motor housing. The motor bearings were seeded with single-point faults of varying diameters (0.007, 0.014, 0.021, and 0.028 inches) using Electro-Discharge Machining (EDM). Faults were introduced independently at three critical components: the inner raceway, the rolling element (ball), and the outer raceway. Vibration signals were recorded for each fault state and for healthy baseline bearings. The motor load was varied from 0 to 3 horsepower (corresponding to motor speeds of approximately 1797 to 1720 RPM) to simulate different operational conditions. The dataset provides time-domain vibration data, typically sampled at 12 kHz or 48 kHz for most studies.

The primary variables documented in the dataset include the fault state (encompassing normal/healthy bearings, inner race faults, ball faults, and outer race faults), the fault diameter (which ranges from 0.007 to 0.028 inches), and the motor load condition (0, 1, 2, and 3 horsepower). Data was captured from accelerometers at multiple sensor positions, namely at the drive end, fan end, and on the base. The motor speed, which correlates directly with the load, is also provided with values of approximately 1797 RPM for 0 hp, 1772 RPM for 1 hp, 1750 RPM for 2 hp, and 1730 RPM for 3 hp. This dataset is a fundamental resource for research in predictive maintenance, condition monitoring, and fault diagnosis. It is specifically designed for developing and testing machine learning and signal processing techniques for the classification and identification of mechanical faults in rotating machinery.

4.2. Data Splitting

The CWRU bearing fault dataset was systematically partitioned into four distinct scenarios following a leave-one-load-out cross-validation approach to evaluate model generalization across varying mechanical load conditions. We worked with the signals recorded at the driven end position sampled at 12 kHz. The samples in both the train and test subsets represent fixed-length samples (segments) that contain the peaks extracted from the signals of each subset. One single signal cannot be used in both subset; i.e. that all samples of the same signal should be in only one subset (train or test). The fragment length of 1000 points (approx. 0.083 seconds at 12 kHz) was chosen to be long enough to capture the entire impulse response of a bearing fault, including subsequent resonances, while remaining short enough to be computationally efficient and focused on the peak event. CWRU dataset splitting scenarios at 12 kHz sampling rate shown in Table 1.

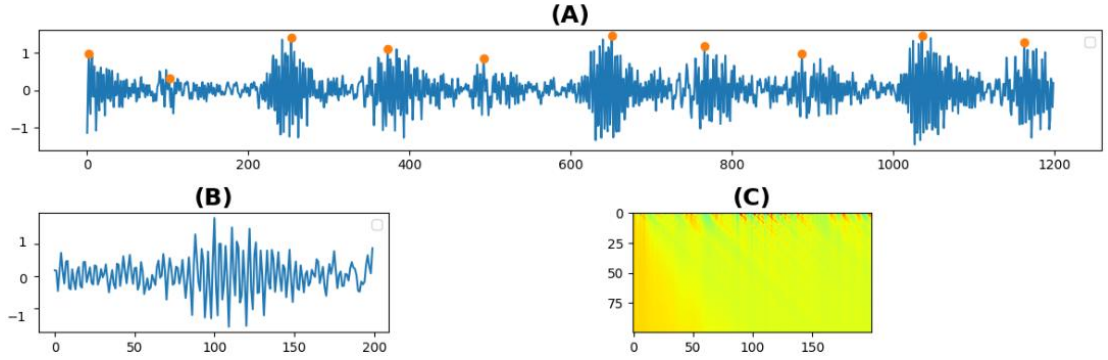

Fig. 1. Peak extraction and PMAT transform from drive end signal

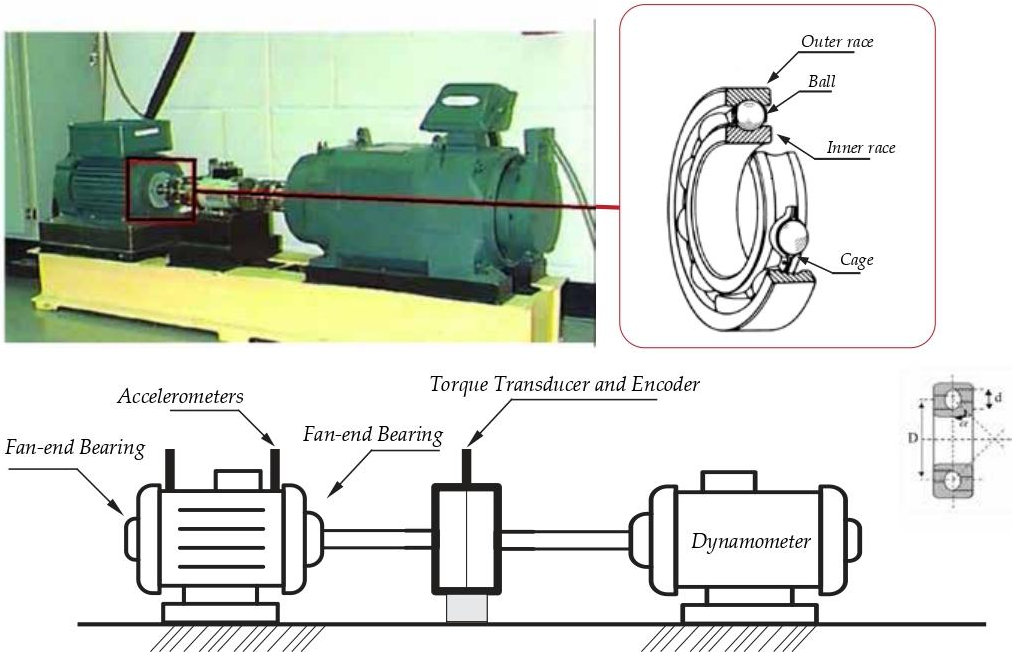

Fig. 2. An Experimental platform of the CWRU bearing test used for generating fault vibration data [5]

Table 1. CWRU dataset splitting scenarios at 12 kHz sampling rate

Scenario	Subsets	Loads	Samples	Test/Train
1	DS1 (Train) DS2 (Test	1,2,3 0	47,114 11,702	24,8%
2	DS3 (Train) DS4 (Test	0,2,3 1	43,410 15,406	35,5%
3	DS5 (Train) DS6 (Test)	0,1,3 2	42,734 16,082	37.6%
4	DS7 (Train) DS8 (Test)	0,1,2 3	43,190 15,626	36,2%

4.3. Scenario Specifications

Scenario 1. The training set (DS1) contains 47,114 samples distributed across loads (1,2,3), while the testing set (DS2) includes 11,702 samples at load 0. The test-to-train ratio is 24.8%, making this the most conservative split with the smallest testing proportion. The distribution of samples across the four classes (Normal, REF, IRF, ORF) is relatively balanced between training and testing subsets. Scenario 2. In this case, DS3 (train) provides 43,410 samples from loads (0,2,3), while DS4 (test) adds 15,406 samples at load 1. The test-to-train ratio reaches 35.5%, indicating a higher proportion of testing samples compared to Scenario 1. Class proportions are well preserved between subsets. Scenario 3. Here, DS5 (train) contributes 42,734 samples under loads (0,1,3), and DS6 (test) provides 16,082 samples under load 2. The resulting test-to-train ratio is 37.6 %, which is the highest among all scenarios. This configuration offers a strong evaluation setting by exposing the model to unseen load 2 during testing. Scenario 4. The training dataset DS7 contains 43,190 samples from loads (0,1,2), while DS8 (test) includes 15,626 samples at load 3. The test-to-train ratio is 36.2 %, similar to Scenario 2. This scenario evaluates generalization at load 3 and provides a balanced distribution across classes.

4.4. Convolutional Neural Network Architecture and the Method Overview

The overview of our method is shown in Fig. 3. The CNN architecture adopted in this study follows the proven design from the original PMAT publication [12], where it demonstrated optimal compatibility with PMAT-transformed signals. This strategic choice, made with input from one of PMAT's original developers, ensures architectural coherence while maintaining consistency with established practices. Our method consists of three main steps:

- Step 1: Use LMPAT to convert the extracted fixed-length fragments of the bearing signal into square 2D images of size 120 × 120.
- Step 2: Use 2D-CNN layers to extract 128 features from the transformed images.
- Step 3: Use the 128 extracted features from Step 2 to classify the corresponding bearing signal fragment into one of the four classes.

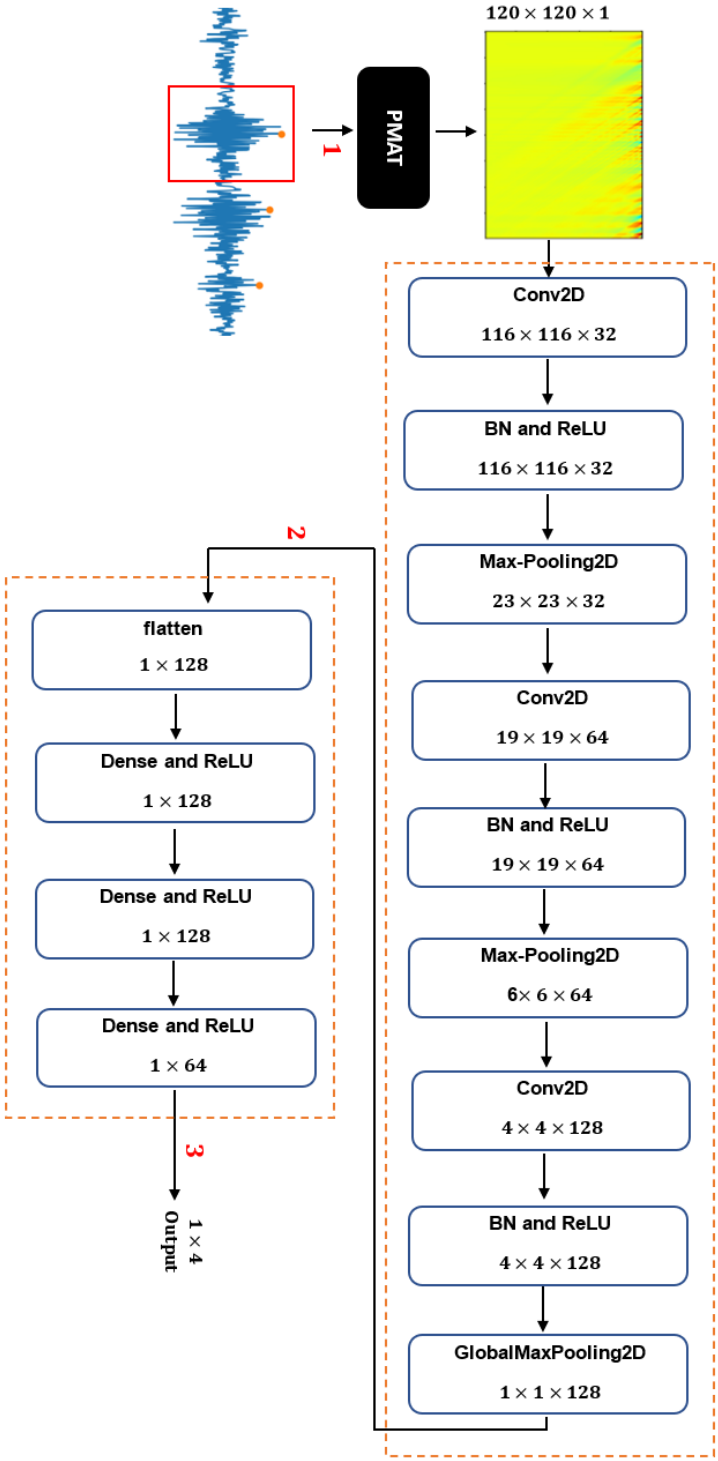

Fig. 3. Flowchart and overview of the approach

The parameters of the used CNN model architecture are given in Table 2,

Table 2. 2D-CNN model layers and parameters

No	Layer name	Kernal size	Filter	Padding	Stride	Output shape
1	Input*	-	-	-	-	120 × 120 × 1
2	Conv2D	5 × 5	32	0	1	116 × 116 × 32
3	BatchNorm2d	-	-	-	-	116 × 116 × 32
4	ReLU	-	-	-	-	116 × 116 × 32
5	MaxPool2D	5 × 5	-	-	5	23 × 23 × 32
6	Conv2D	5 × 5	64	0	1	19 × 19 × 64
7	BatchNorm2d	-	-	-	-	19 × 19 × 64
8	ReLU	-	-	-	-	19 × 19 × 64
9	MaxPool2D	3 × 3	-	-	3	6 × 6 × 64
10	Conv2D	3 × 3	128	0	1	4 × 4 × 128
11	BatchNorm2d	-	-	-	-	4 × 4 × 128
12	ReLU	-	-	-	-	4 × 4 × 128
13	AMaxPool2d**	-	-	-	-	1 × 1 × 128
14	Flatten	-	-	-	-	1 × 128
15	Flatten	-	-	-	-	1 × 128
16	Flatten	-	-	-	-	1 × 64
17	Flatten	-	-	-	-	1 × 4

* The input refers to the PMAT transformed bearing signal fragment of size 120 × 120,
** AMaxPool2d is the Adaptive Max Pooling layer.

4.5. Implementation Details

The model was trained with a batch size of 512 on an NVIDIA Tesla P100 GPU provided freely by Kaggle [13]. Training was performed over 20 epochs using the Adam optimizer with a learning rate of 0.02.

5. Results and Discussion

The bearing fault classification system was evaluated under four load conditions using a leave-one-load-out cross-validation scheme. The resulting confusion matrices and performance metrics reveal distinct patterns across the tested scenarios. In Scenario 1 (Test Load 0), corresponding to the no-load condition, the model achieved a macro-averaged F1-score of 86.94%. While the class (REF) exhibited a high recall (99.50%), its precision was relatively low (56.90%), indicating a notable rate of false positives for rolling element faults. This reduced performance can be attributed to the weak fault signatures present in the absence of load, as mechanical stresses that amplify defect-related vibrations are minimal. Consequently, fault-related frequency components overlap more strongly with background noise, leading to reduced discriminability. In contrast, under loaded conditions (Section 2.3), the model demonstrated near-perfect classification performance. Specifically, Scenario 2 (Test Load 1) achieved a macro F1-score of 99.83%, with precision and recall exceeding 99.60% for all fault classes. Scenario 3 (Test Load 2) further improved performance, reaching a macro F1-score of 99.95%, while Scenario 4 (Test Load 3) yielded a similar result of 99.91%. The consistent improvement observed under increasing load levels confirms that the fault-induced vibration patterns become more distinct as the applied load increases, enhancing the separability of the feature representations extracted by the PMAT–2D-CNN framework.

Across all experiments, the REF class exhibited the highest variability in classification performance, reflecting its sensitivity to operating conditions and the potential overlap of healthy and incipient fault patterns. Nevertheless, the overall results demonstrate that the proposed model generalizes effectively to unseen load conditions. Furthermore, the specificity remained consistently high (more than 99%) across most scenarios, highlighting the robustness of the classifier in correctly identifying non-fault cases. These findings suggest that the PMAT-based representation, coupled with the 2D-CNN architecture, effectively captures the discriminative temporal–spectral features necessary for reliable fault detection under varying mechanical loads. Fig. 4 and Fig. 5 summarize the confusion matrices and receiver operating characteristic (ROC) curves corresponding to these experiments. The four scenarios. The results, together with the AUC values, with values ranging

from 0.99 to 1.00, reported in Table 3, demonstrate the robustness of the model, achieving strong performance across all classes.

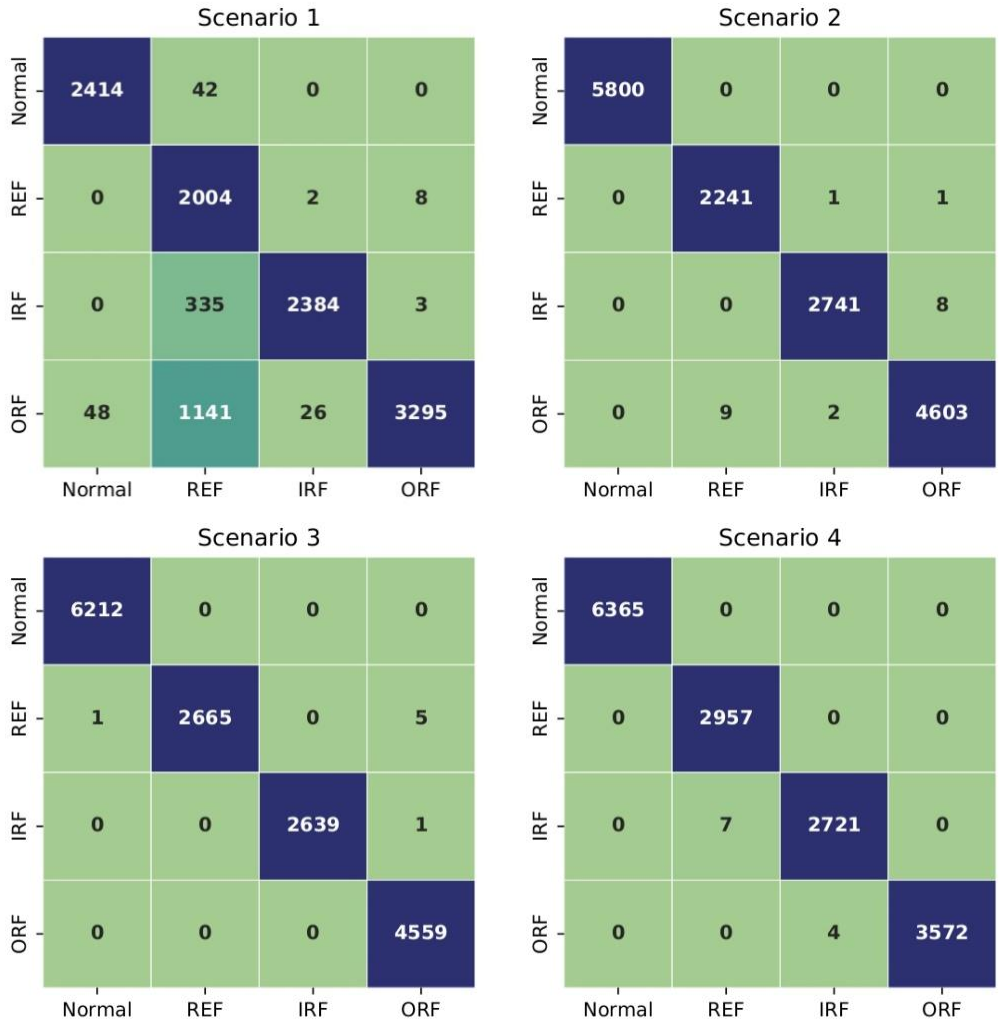

Fig. 4. Performance results across all four testing scenarios showing confusion matrices

5.1. Comparison with Continuous Wavelet Transform

In this section, we compare our method using an alternative transform which is the Continuous Wavelet Transform (CWT) instead of PMAT transform. We have repeated the same scenarios described in section 3.3 within the same framework presented in section 3.4 replacing PMAT by CWT transform. CWT employs a wavelet, which is a small wave-like function, to generate a time-scale scalogram from a signal. The wavelet is systematically scaled and shifted across the signal over time to capture information at various times and scales. The comparison is done based on four metrics Accuracy and the macro average of the precision, recall, and the F1-score.

The comparative results, presented in Table 4, indicate that CWT achieves superior performance in Scenario 1 (Load 0), whereas PMAT consistently out-performs CWT in the other scenarios. This behavior can be explained by the nature of the analyzed signals. Under zero-load conditions, fault signatures are weak and localized, and the multi-resolution capability of CWT is more effective in capturing such subtle, transient variations around the peaks. In contrast, when loads are applied, the peaks become more distinctive and the local fault-related features gain stronger energy, which enhances the effectiveness of PMAT. By relying on progressive averaging in the time domain before converting to a scalogram, PMAT is able to highlight these localized fault signatures while suppressing noise, leading to its superior performance under loaded conditions.

5.2. Analysis of PMAT's Performance Characteristics

The performance disparity between loaded and non-load conditions reveals a fundamental aspect of our peak-centric approach. Under motor load, impact on bearings generates distinct strong peaks that PMAT effectively enhances. In no-load conditions (Scenario 1), these impacts are less energetic, resulting in weaker peaks that provide less discriminative information for the PMAT transform. This explains the particular difficulty with REF faults under no-load, as ball faults inherently produce more chaotic and lower-energy signatures compared to inner or outer race faults. This finding establishes that PMAT's effectiveness is contingent on the presence of well-defined transient events, positioning it as an ideal tool for loaded industrial scenarios while highlighting a limitation for very low-load applications.

Table 3. Performance results of bearing fault classification across four testing scenarios using leave-one-load-out cross-validation

Scenario	Class	Precision	Recall	Specificity	F1-score	AUC	Accuracy
	Normal	98.05%	98.29%	99.46%	98.17%	1.00	
	REF	56.90%	99.50%	99.88%	72.40%	1.00	
1	IRF	98.84%	87.58%	95.81%	92.87%	1.00	86.28%
	ORF	99.67%	73.06%	84.84%	84.31%	0.98	
	Macro avg	**88.36%**	**89.61%**	**95.00%**	**86.94%**	**0.99**	
	Normal	100.00%	100.00%	100.00%	100.00%	1.00	
	REF	99.60%	99.91%	99.98%	99.76%	1.00	
2	IRF	99.89%	99.71%	99.94%	99.80%	1.00	99.86%
	ORF	99.80%	99.76%	99.90%	99.78%	1.00	
	Macro avg	**99.82%**	**99.85%**	**99.96%**	**99.83%**	**1.00**	
	Normal	99.98%	100.00%	100.00%	99.99%	1.00	
	REF	100.00%	99.78%	99.96%	99.89%	1.00	
3	IRF	100.00%	99.96%	99.99%	99.98%	1.00	99.96%
	ORF	99.87%	100.00%	100.00%	99.93%	1.00	
	Macro avg	**99.96%**	**99.93%**	**99.99%**	**99.95%**	**1.00**	
	Normal	100.00%	100.00%	100.00%	100.00%	1.00	
	REF	99.76%	100.00%	100.00%	99.88%	1.00	
4	IRF	99.85%	99.74%	99.95%	99.80%	1.00	99.93%
	ORF	100.00%	99.89%	99.97%	99.94%	1.00	
	Macro avg	**99.90%**	**99.91%**	**99.98%**	**99.91%**	**1.00**	

Table 4. Comparison between PMAT and CWT methods across four scenarios

Method	Scenario	Accuracy	M.avg Precision	M.avg Recall	M.avg F1
PMAT	1	86.28%	88.36%	89.61%	86.94%
	2	99.86%	99.82%	99.85%	99.83%
	3	99.96%	99.96%	99.93%	99.95%
	4	99.93%	99.90%	99.91%	99.91%
CWT	1	97.31%	97.69%	97.38%	97.52%
	2	97.44%	96.85%	97.64%	97.15%
	3	97.92%	98.28%	96.83%	97.43%
	4	99.00%	98.93%	98.59%	98.73%

5.3. Performance Comparison (Acc \%) with Other Published Works

Table 5 summarizes a comparison between our method which is implemented based on PMAT transform and 2D-CNN neural network and other recent method implemented using different techniques. As shown in Table 5, our method achieves competitive state-of-the-art performance. The superior results under loaded conditions compared to methods like CWT-based approaches [6] and Graph-based approach [2] suggest that PMAT's peak-enhancement capability provides a more discriminative representation when fault signatures are strong. It is also superior to conventional CNN- or DCNN-based methods [4] and [6]. Although some studies such as Wen et al. [21] reported slightly higher accuracy (99.8%), the proposed PMAT + 2D-CNN framework demonstrates state of the art performance overall loaded conditions, confirming its effectiveness and robustness

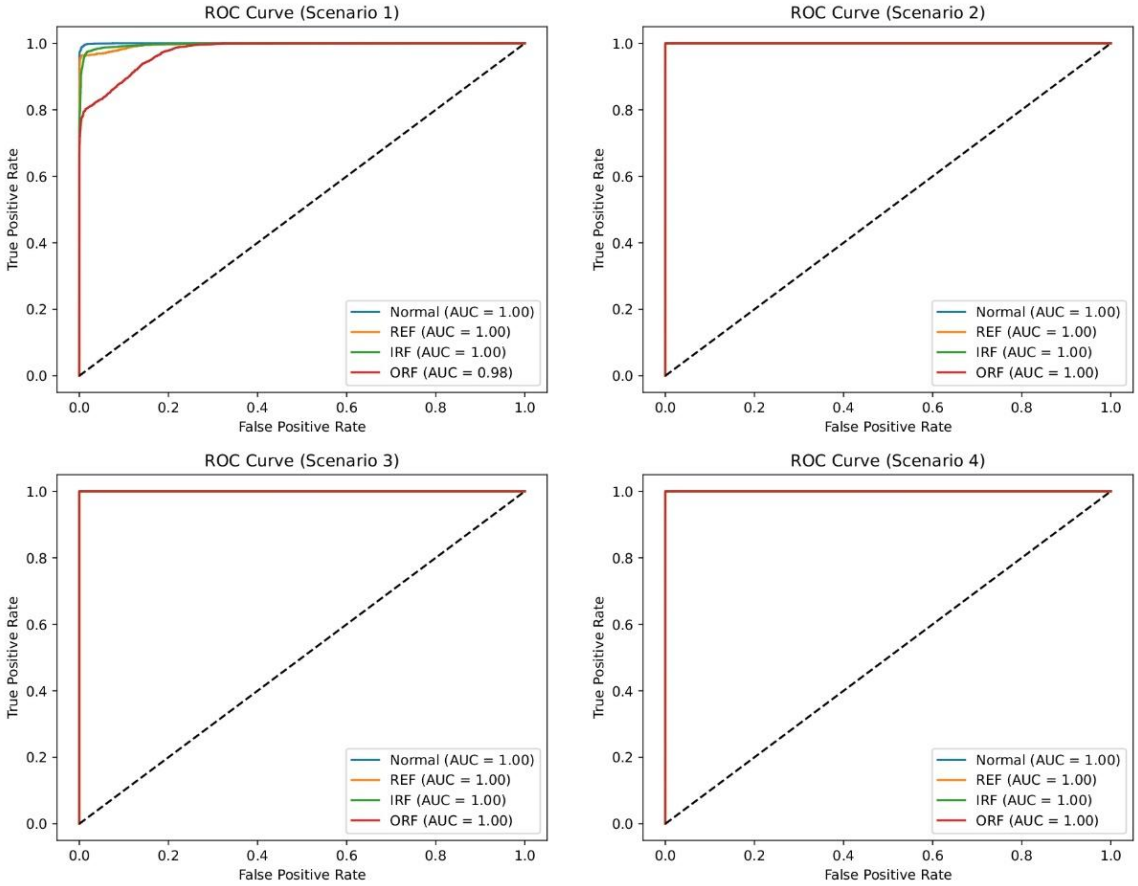

Fig. 5. Performance results across all four testing scenarios showing ROC

Table 5. Comparison of the results obtained by our method with other works

Paper / Source	Year	Key Technique Used	Accuracy
Proposed method	2025	PMAT transform and 2D-CNN	99.96%
Alqunun et al. [13]	2025	ResNet-50, SVM, CWT	95.51%
Y. Zhang et al. [14]	2025	MLSCA-CW Network	92.02%
Chen, et al. [2]	2024	GraphSAGE, Graph Aggregation	99.53%
K. Tran, et al. [15]	2024	Robust-MBFD	90.0%
O.ali et al. [16]	2023	EWC Algorithm	97.06%
Yuan, et al. [6]	2020	CWT, CNN, SVM	98.75%
Han.K et al. [17]	2024	CNN-LSTM-GRU	92.5%
H. Wang et al. [18]	2022	VGG-16	98.9%
A. Shenfield et al. [4]	2020	DCNN	99.1%
C. Zhang et al. [19]	2019	VAE	98.06%
L. Shao et al. [21]	2019	DNN	97.4%
Wen et al. [20]	2018	CNN-LeNet	99.8%

6. Conclusion and Future Work

This study presented a comprehensive validation of the Progressive Moving Average Transform (PMAT) for mechanical fault diagnosis, successfully demonstrating its generalization from the biomedical to industrial domains. The novel peak-centric framework, which combines PMAT with a purpose-built 2D-CNN, establishes a new paradigm for bearing fault classification by concentrating computational resources on the most informative signal regions—the impact peaks where fault signatures are most pronounced. The method's exceptional performance, achieving more than 99.8\% accuracy and macro F1-scores across three loaded scenarios, underscores its robustness and strong generalization capability to unseen operational conditions. This positions PMAT as a highly effective

transformation technique for industrial applications where bearings operate under typical load conditions.

However, our rigorous evaluation also revealed a fundamental characteristic of the peak-dependent approach: performance under no-load conditions (Scenario 1) was notably lower, particularly for rolling element faults. This limitation is intrinsic to PMAT's design principle—its effectiveness is contingent upon the presence of distinct energetic peaks, which are attenuated in low-load scenarios. Rather than a methodological flaw, this finding provides crucial insight for practitioners: PMAT excels in loaded industrial environments, but may require supplementation for very low-load applications.

The comparative analysis with Continuous Wavelet Transform further validated this understanding, showing complementary strengths where CWT's multi-resolution capability better handles subtle signatures in no-load conditions, while PMAT's progressive averaging more effectively enhances localized fault features under load. In future work, we plan to develop Hybrid PMAT-CWT framework integrated transformation that leverages CWT's multi-resolution analysis for comprehensive feature capture and PMAT's peak-enhancement for focused fault signature amplification, creating a universally robust solution across all operational conditions.

Data and Code Availability: To ensure complete reproducibility, facilitate further research, and promote transparent scientific discourse, the complete source code and data for this study have been made publicly available on the Zenodo platform https://doi.org/10.5281/zenodo.17548767.

Author Contribution: All authors contributed equally to the main contributor to this paper. All authors read and approved the final paper.

Funding: This research received no external funding.

Conflicts of Interest: The authors declare no conflict of interest.

References

[1] Y. Wang, D. Li, L. Li, R. Sun, and S. Wang, "A novel deep learning framework for rolling bearing fault diagnosis enhancement using VAE-augmented CNN model," *Heliyon*, vol. 10, no. 15, p. e29044, 2024, https://doi.org/10.1016/j.heliyon.2024.e35407.

[2] J. Chen, X. Du, Y. Qian, and G. Jeon, "Bearing Fault Diagnosis using Graph Sampling and Aggregation Network," *arXiv*, 2024, https://doi.org/10.48550/arXiv.2408.07099.

[3] T. Zhang, S. Liu, Y. Wei, and H. Zhang, "A novel feature adaptive extraction method based on deep learning for bearing fault diagnosis," *Measurement*, vol. 185, p. 110030, 2021, https://doi.org/10.1016/j.measurement.2021.110030.

[4] A. Shenfield and M. Howarth, "A novel deep learning model for the detection and identification of rolling element-bearing faults," *Sensors*, vol. 20, no. 18, p. 5112, 2020, https://doi.org/10.3390/s20185112.

[5] D. Neupane and J. Seok, "Bearing Fault Detection and Diagnosis Using Case Western Reserve University Dataset With Deep Learning Approaches: A Review," *IEEE Access*, vol. 8, pp. 93155-93178, 2020, https://doi.org/10.1109/ACCESS.2020.2990528.

[6] L. Yuan, D. Lian, X. Kang, Y. Chen, and K. Zhai, "Rolling bearing fault diagnosis based on convolutional neural network and support vector machine," *IEEE Access*, vol. 8, pp. 137395-137406, 2020, https://doi.org/10.1109/ACCESS.2020.3011411.

[7] Q. Wang, B. Wu, P. Zhu, P. Li, W. Zuo, and Q. Hu, "ECA-Net: Efficient channel attention for deep convolutional neural networks," *Proceedings of the IEEE/CVF Conference on Computer Vision and Pattern Recognition*, vol. 2020, pp. 11534-11542, 2020, https://doi.org/10.1109/CVPR42600.2020.01155.

[8] A. Kiakojouri and L. Wang, "A generalized convolutional neural network model trained on simulated data for fault diagnosis in a wide range of bearing designs," *Sensors*, vol. 25, no. 8, p. 2378, 2025, https://doi.org/10.3390/s25082378.

[9] Y. Zeng, J. Liu, Y. Long, Z. Shen, and J. Liang, "A Deep Learning-Based Bearing Fault Diagnosis Model: IEMDWave-SwinTGAMNet," *2024 8th International Conference on Electrical, Mechanical and Computer Engineering (ICEMCE)*, pp. 1325-1332, 2024, https://doi.org/10.1109/ICEMCE64157.2024.10862037.

[10] M. Al-Sa'd, T. Jalonen, S. Kiranyaz, and M. Gabbouj, "Quadratic Time-Frequency Analysis of Vibration Signals for Diagnosing Bearing Faults," *arXiv*, 2024, https://doi.org/10.48550/arXiv.2401.01172.

[11] I. Raouf, H. Lee, Y. R. Noh, B. D. Youn, and H. S. Kim, "Prognostic health management of the robotic strain wave gear reducer based on variable speed of operation: A data-driven via deep learning approach," *Journal of Computational Design and Engineering*, vol. 9, no. 5, pp. 1775-1788, 2022, https://doi.org/10.1093/jcde/qwac091.

[12] R. Mokhtari, S. Brahim Belhouari, K. Kassoul, and A. Hocini, "ECG heartbeat classification using progressive moving average transform," *Scientific Reports*, vol. 15, no. 1, p. 4285, 2025, https://doi.org/10.1038/s41598-025-88119-9.

[13] Banachewicz, Konrad, and L. Massaron, "The Kaggle Book: Data analysis and machine learning for competitive data science," *Packt Publishing Ltd*, 2022, https://books.google.co.id/books?id=GAVsEAAAQBAJ&dq=Kaggle:+Your+machine+learning+and+data+science+community&lr=&source=gbs_navlinks_s.

[14] K. Alqunun *et al*., "An efficient bearing fault detection strategy based on a hybrid machine learning technique," *Scientific Reports*, vol. 15, no. 1, p. 18739, 2025, https://doi.org/10.1038/s41598-025-75708-6.

[15] Y. Zhang, L. Lin, J. Wang, W. Zhang, S. Gao, and Z. Zhang, "Attention activation network for bearing fault diagnosis under various noise environments," *Scientific Reports*, vol. 15, no. 1, p. 977, 2025, https://doi.org/10.1038/s41598-025-85275-w.

[16] K. Tran, L. Pham, V.-R. Nguyen, and H.-S.-H. Nguyen, "A robust deep learning system for motor bearing fault detection: leveraging multiple learning strategies and a novel double loss function," *Signal, Image and Video Processing*, vol. 19, no. 4, pp. 1-11, 2025, https://doi.org/10.1007/s11760-025-03848-8.

[17] O. M. A. Ali, R. A. Hamaamin, and S. W. Kareem, "Deep Learning Techniques for Early Fault Detection in Bearings: An Intelligent Approach," *Kurdistan Journal of Applied Research*, vol. 10, no. 1, pp. 18-34, 2025, https://doi.org/10.24017/science.2025.1.2.

[18] K. Han, W. Wang, and J. Guo, "Research on a Bearing fault diagnosis method based on a CNN-LSTM-GRU model," *Machines*, vol. 12, no. 12, p. 927, 2024, https://doi.org/10.3390/machines12120927.

[19] H. Wang, W. Sun, L. He, and J. Zhou, "Rolling bearing fault diagnosis using multi-sensor data fusion based on 1D-CNN model," *Entropy*, vol. 24, no. 5, p. 573, 2022, https://doi.org/10.3390/e24050573.

[20] S. Zhang, F. Ye, B. Wang, and T. G. Habetler, "Semi-supervised learning of bearing anomaly detection via deep variational autoencoders," *arXiv*, 2019, https://doi.org/10.48550/arXiv.1912.01096.

[21] L. Wen, X. Li, L. Gao and Y. Zhang, "A New Convolutional Neural Network-Based Data-Driven Fault Diagnosis Method," *IEEE Transactions on Industrial Electronics*, vol. 65, no. 7, pp. 5990-5998, 2018, https://doi.org/10.1109/TIE.2017.2774777.

[22] V.-C. Nguyen, D.-T. Hoang, X.-T. Tran *et al*., "A Bearing Fault Diagnosis Method Using Multi-Branch Deep Neural Network," *Machines*, vol. 9, no. 12, p. 345, 2021, https://doi.org/10.3390/machines9120345.

[23] Y. Chen, D. Zhang, H. Zhang and Q. -G. Wang, "Dual-Path Mixed-Domain Residual Threshold Networks for Bearing Fault Diagnosis," *IEEE Transactions on Industrial Electronics*, vol. 69, no. 12, pp. 13462-13472, 2022, https://doi.org/10.1109/TIE.2022.3144572.

[24] B. Yang, R. Liu and E. Zio, "Remaining Useful Life Prediction Based on a Double-Convolutional Neural Network Architecture," *IEEE Transactions on Industrial Electronics*, vol. 66, no. 12, pp. 9521-9530, 2019, https://doi.org/10.1109/TIE.2019.2924605.

[25] W. Zhang, C. Li, G. Peng, Y. Chen, and Z. Zhang, "A deep convolutional neural network with new training methods for bearing fault diagnosis under noisy environment and different working load," *Mechanical Systems and Signal Processing*, vol. 100, pp. 439-453, 2018, https://doi.org/10.1016/j.ymssp.2017.06.022.

[26] Z. Chen, K. Gryllias, and W. Li, "Intelligent fault diagnosis for rotary machinery using transferable convolutional neural networks," *IEEE Transactions on Industrial Informatics*, vol. 16, no. 1, pp. 339-349, 2020, https://doi.org/10.1109/TII.2019.2917233.

[27] R. Liu, B. Yang, E. Zio, and X. Chen, "Artificial intelligence for fault diagnosis of rotating machinery: A review," *Mechanical Systems and Signal Processing*, vol. 108, pp. 33-47, 2018, https://doi.org/10.1016/j.ymssp.2018.02.016.

[28] H. Wang, Z. Liu, D. Peng, and Y. Qin, "Understanding and learning discriminant features based on multiattention 1DCNN for wheelset bearing fault diagnosis," *IEEE Transactions on Industrial Informatics*, vol. 16, no. 9, pp. 5735-5745, 2020, https://doi.org/10.1109/TII.2019.2955540.

[29] L. Wen, L. Gao, and X. Li, "A new deep transfer learning based on sparse auto-encoder for fault diagnosis," *IEEE Transactions on Systems, Man, and Cybernetics: Systems*, vol. 49, no. 1, pp. 136-144, 2019, https://doi.org/10.1109/TSMC.2017.2754287.

[30] J. Cen, Z. Yang, X. Liu, J. Xiong, and H. Chen, "A Review of Data-Driven Machinery Fault Diagnosis Using Machine Learning Algorithms," *Journal of Vibration Engineering & Technologies*, vol. 10, no. 7, pp. 2481–2507, 2022, https://doi.org/10.1007/s42417-022-00498-9.

[31] M. Zhao, S. Zhong, X. Fu, B. Tang, and M. Pecht, "Deep residual networks with adaptively parametric rectifier linear units for fault diagnosis," *IEEE Transactions on Industrial Electronics*, vol. 68, no. 3, pp. 2587-2597, 2021, https://doi.org/10.1109/TIE.2020.2972458.

[32] Y. Lei, B. Yang, X. Jiang, F. Jia, N. Li, and A. K. Nandi, "Applications of machine learning to machine fault diagnosis: A review and roadmap," *Mechanical Systems and Signal Processing*, vol. 138, p. 106587, 2020, https://doi.org/10.1016/j.ymssp.2019.106587.

[33] Y. Zou, Y. Liu, J, Deng, Y. Jiang, W. Zhang, "A novel transfer learning method for bearing fault diagnosis under multiple working conditions," *Measurement*, vol. 171, p. 108767, 2021, https://doi.org/10.1016/j.measurement.2020.108767.

[34] Y. Xu *et al*., "A Hybrid Deep-Learning Model for Fault Diagnosis of Rolling Bearings," *Measurement*, vol. 169, p. 108502, 2021, https://doi.org/10.1016/j.measurement.2020.108502.

[35] P. Ma, H. Zhang, W. Fan, C. Wang, G. Wen, and X. Zhang, "A Novel Bearing Fault Diagnosis Method Based on 2D Image Representation and Transfer Learning-Convolutional Neural Network," *Measurement Science and Technology*, vol. 30, no. 5, p. 055402, 2019, https://doi.org/10.1088/1361-6501/ab0793.

[36] X. Chen, R. Yang, Y. Xue, M. Huang, R. Ferrero and Z. Wang, "Deep Transfer Learning for Bearing Fault Diagnosis: A Systematic Review Since 2016," *IEEE Transactions on Instrumentation and Measurement*, vol. 72, pp. 1-21, 2023, https://doi.org/10.1109/TIM.2023.3244237.

[37] Y. Zhou, Z. Lei, G. Wen, Y. Su, and Z. Zhang, "MSC-APFNN: Fault Diagnosis Deep Transfer Network for Rotating Machine based on Multi-scale Convolutional Extraction and Adaptive Pruning Fuzzy Inference System," *International Conference on Artificial Intelligence and Autonomous Transportation*, pp 310-324, 2024, https://doi.org/10.1007/978-981-96-3969-4_35.

[38] X. Jin, M. Zhao, T. W. S. Chow and M. Pecht, "Motor Bearing Fault Diagnosis Using Trace Ratio Linear Discriminant Analysis," *IEEE Transactions on Industrial Electronics*, vol. 61, no. 5, pp. 2441-2451, 2014, https://doi.org/10.1109/TIE.2013.2273471.

[39] S. Mushtaq, M. M. Islam, and M. Sohaib, "Deep learning aided data-driven fault diagnosis of rotatory machine: A comprehensive review," *Energies*, vol. 14, no. 16, p. 5150, 2021, https://doi.org/10.3390/en14165150.

[40] X. Zhang, B. Zhao, and Y. Lin, "Machine Learning Based Bearing Fault Diagnosis Using the Case Western Reserve University Data: A Review," *IEEE Access*, vol. 9, pp. 155598–155608, 2021, https://doi.org/10.1109/ACCESS.2021.3128669.

[41] V. Barai *et al*., S. M. Ramteke, V. Dhanalkotwar, Y. Nagmote, S. Shende, and D. Deshmukh, "Bearing Fault Diagnosis Using Signal Processing and Machine Learning Techniques: A Review," in *IOP Conference Series: Materials Science and Engineering*, vol. 1259, no. 1, p. 012034, 2022, https://doi.org/10.1088/1757-899X/1259/1/012034.

[42] C. V. Jaarsveldt, G. W. Peters, M. Ames and M. Chantler, "Tutorial on Empirical Mode Decomposition: Basis Decomposition and Frequency Adaptive Graduation in Non-Stationary Time Series," *IEEE Access*, vol. 11, pp. 94442-94478, 2023, https://doi.org/10.1109/ACCESS.2023.3307628.

[43] M. Hakim, A. A. B. Omran, A. N. Ahmed, M. Al-Waily, and A. Abdellatif, "A Systematic Review of Rolling Bearing Fault Diagnoses Based on Deep Learning and Transfer Learning: Taxonomy, Overview, Application, Open Challenges, Weaknesses and Recommendations," *Ain Shams Engineering Journal*, vol. 14, no. 4, p. 101945, 2023, https://doi.org/10.1016/j.asej.2022.101945.

[44] M. Ye, X. Yan, and M. Jia, "Rolling Bearing Fault Diagnosis Based on VMD-MPE and PSO-SVM," *Entropy*, vol. 23, no. 6, p. 762, 2021, https://doi.org/10.3390/e23060762.

[45] A. Anwarsha and T. N. Babu, "A Review on the Role of Tunable Q-Factor Wavelet Transform in Fault Diagnosis of Rolling Element Bearings," *Journal of Vibration Engineering & Technologies*, vol. 10, no. 5, pp. 1793–1808, 2022, https://doi.org/10.1007/s42417-022-00484-1.

[46] A. Anwarsha and N. B. T, "Fault detection of taper roller bearings using tunable Q-factor wavelet transform and fault classification using long–short-term memory network," *Scientific Reports*, vol. 15, no. 1, p. 9672, 2025, https://doi.org/10.1038/s41598-025-93514-3.

[47] M. Cerrada, R.-V. Sánchez, C. Li, F. Pacheco, D. Cabrera, J. V. De Oliveira, and R. E. Vásquez, "A Review on Data-Driven Fault Severity Assessment in Rolling Bearings," *Mechanical Systems and Signal Processing*, vol. 99, pp. 169-196, 2018, https://doi.org/10.1016/j.ymssp.2017.06.012.

[48] T. Han, C. Liu, W. Yang, and D. Jiang, "A novel adversarial learning framework in deep convolutional neural network for intelligent diagnosis of mechanical faults," *Knowledge-Based Systems*, vol. 165, pp. 474-487, 2019, https://doi.org/10.1016/j.knosys.2018.12.019.

[49] S. Panigrahi, A. Nanda, T. Swarnkar, "A survey on transfer learning, Intelligent and Cloud Computing: Proceedings of ICICC 2019," pp. 781-789, 2020, https://books.google.co.id/books/about/Intelligent_and_Cloud_Computing.html?id=amMGEAAAQBAJ&redir_esc=y.

[50] Z. Chen and W. Li, "Multisensor feature fusion for bearing fault diagnosis using sparse autoencoder and deep belief network," *IEEE Transactions on Instrumentation and Measurement*, vol. 66, no. 7, pp. 1693-1702, 2017, https://doi.org/10.1109/TIM.2017.2669947.

[51] J. Dai, J. Wang, W. Huang, J. Shi, and Z. Zhu, "Machinery Health Monitoring Based on Unsupervised Feature Learning via Generative Adversarial Networks," *IEEE/ASME Transactions on Mechatronics*, vol. 25, no. 5, pp. 2252-2263, 2020, https://doi.org/10.1109/TMECH.2020.3012179.

[52] H. Liu, J. Zhou, Y. Zheng, W. Jiang, and Y. Zhang, "Fault diagnosis of rolling bearings with recurrent neural network-based autoencoders," *ISA Transactions*, vol. 77, pp. 167-178, 2018, https://doi.org/10.1016/j.isatra.2018.04.005.

[53] O. Janssens *et al.*, "Convolutional neural network based fault detection for rotating machinery," *Journal of Sound and Vibration*, vol. 377, pp. 331-345, 2016, https://doi.org/10.1016/j.jsv.2016.05.027.

[54] B. Yang, Y. Lei, F. Jia, and S. Xing, "An intelligent fault diagnosis approach based on transfer learning from laboratory bearings to locomotive bearings," *Mechanical Systems and Signal Processing*, vol. 122, pp. 692-706, 2019, https://doi.org/10.1016/j.ymssp.2018.12.051.

[55] K. He, X. Zhang, S. Ren and J. Sun, "Deep Residual Learning for Image Recognition," *2016 IEEE Conference on Computer Vision and Pattern Recognition (CVPR)*, pp. 770-778, 2016, https://doi.org/10.1109/CVPR.2016.90.

[56] Y. Dong, J. B. Cordonnier, and A. Loukas, "Attention is not all you need: Pure attention loses rank doubly exponentially with depth," *Proceedings of the 38th International Conference on Machine Learning (ICML)*, vol. 139, pp. 2793-2803, 2021, https://proceedings.mlr.press/v139/dong21a.html.

[57] C. Li, J. Xiong, X. Zhu, Q. Zhang, and S. Wang, "Fault Diagnosis Method Based on Encoding Time Series and Convolutional Neural Network," *IEEE Access*, vol. 8, pp. 165232-165246, 2020, https://doi.org/10.1109/ACCESS.2020.3021007.

[58] R. Zhao, R. Yan, Z. Chen, K. Mao, P. Wang, and R. X. Gao, "Deep learning and its applications to machine health monitoring," *Mechanical Systems and Signal Processing*, vol. 115, pp. 213-237, 2019, https://doi.org/10.1016/j.ymssp.2018.05.050.

[59] Y. Cheng, M. Lin, J. Wu, H. Zhu, and X. Shao, "Intelligent fault diagnosis of rotating machinery based on continuous wavelet transform-local binary convolutional neural network," *Knowledge-Based Systems*, vol. 216, p. 106796, 2021, https://doi.org/10.1016/j.knosys.2021.106796.

[60] F. Jia, Y. Lei, J. Lin, X. Zhou, and N. Lu, "Deep neural networks: A promising tool for fault characteristic mining and intelligent diagnosis of rotating machinery with massive data," *Mechanical Systems and Signal Processing*, vol. 72, pp. 303-315, 2016, https://doi.org/10.1016/j.ymssp.2015.10.025.